The AAA-ATPase FIGL-1 controls mitotic progression, and its levels are regulated by the CUL-3^{MEL-26} E3 ligase in the *C. elegans* germ line

Sarah Luke-Glaser[1], Lionel Pintard[2,*,‡], Mike Tyers[2] and Matthias Peter[1,‡]

[1]Institute of Biochemistry, HPM G8, ETH Hönggerberg, 8093 Zürich, Switzerland
[2]Samuel Lunenfeld Research Institute, Mount Sinai Hospital, 600 University Avenue, Toronto M5G1X5, Canada
*Present address: Institut Jacques Monod, Université Paris 6 et 7, 2 place Jussieu Tour 43, 75251 Paris CEDEX 05, France
‡Authors for correspondence (e-mails: pintard.lionel@ijm.jussieu.fr; matthias.peter@bc.biol.ethz.ch)

Accepted 10 July 2007
Journal of Cell Science 120, 3179-3187 Published by The Company of Biologists 2007
doi:10.1242/jcs.015883

Summary

Members of the AAA-ATPase (ATPases associated with diverse cellular activities) family use the energy from ATP hydrolysis to disrupt protein complexes involved in many cellular processes. Here, we report that FIGL-1 (Fidgetin-like 1), the single *Caenorhabditis elegans* homolog of mammalian fidgetin and fidgetin-like 1 AAA-ATPases, controls progression through mitosis in the germ line and the early embryo. Loss of *figl-1* function leads to the accumulation of mitotic nuclei in the proliferative zone of the germ line, resulting in sterility owing to depletion of germ cells. Like the AAA-ATPase MEI-1 (also known as katanin), FIGL-1 interacts with microtubules and with MEL-26, a specificity factor of CUL-3-based E3 ligases involved in targeting proteins for ubiquitin-dependent degradation by the 26S proteasome. In the germ line, FIGL-1 is enriched in nuclei of mitotic cells, but it disappears at the transition into meiosis. Conversely, MEL-26 expression is low in nuclei of the mitotic zone and induced during meiosis. FIGL-1 accumulates in the germ line and spreads to the meiotic zone after inactivation of *mel-26* or *cul-3* in vivo. We conclude that degradation of FIGL-1 by the CUL-3^{MEL-26} E3 ligase spatially restricts FIGL-1 function to mitotic cells, where it is required for correct progression through mitosis.

Key words: Ubiquitin-dependent degradation, Germ line, Embryo, Cullin, Fidgetin, Fidgetin-like

Introduction

The development of an organism requires the precise orchestration of cell proliferation, cell differentiation and morphogenesis. Cell proliferation is driven by cyclin-dependent kinases (CDKs) and the ubiquitin-dependent degradation pathway. These activities ensure the orderly progression from DNA replication to mitosis and promote faithful segregation of the duplicated sister chromatids between daughter cells by the mitotic spindle (Nakayama and Nakayama, 2006). Despite considerable progress towards understanding the mechanisms of cell cycle progression in single cells, much less is known about the coordination of cell cycle events and development in a multicellular context.

The nematode *C. elegans* provides a powerful setting in which cell cycle control can be genetically analyzed during development. In particular, studies of the regulation of cell proliferation in the germ line and the asymmetric cell divisions in early embryos have provided important insights into the mechanisms that govern cell division in multicellular organisms. A key step in the development of the germ line is the decision of germ cells to either proliferate or undergo meiotic development (Marston and Amon, 2004). The gonad of *C. elegans* is formed by two 'U-shaped' tubes, each of which contains a syncitium of hundreds of nuclei that can be subdivided into a mitotic zone and a meiotic zone (Kimble and Crittenden, 2005). The mitotic zone is located at the distal end of each tube and contains the mitotic germ cells (Kimble and White, 1981). As germ cells move proximally, they exit the mitotic cycle to enter meiotic prophase, in which the cells have characteristic crescent-shaped nuclei (MacQueen and Villeneuve, 2001). Germ cells that enter meiotic prophase must produce all of the cellular components necessary for meiosis to occur correctly, such as factors that align homologous chromosomes and form the synaptonemal complex (Champion and Hawley, 2002). Translation of many meiotic regulators is repressed in the proliferation zone, thereby ensuring that they cannot interfere with replication or segregation of chromosomes during mitosis. Although germ line proliferation is essential to amplify the germ cells before the onset of meiosis, little is known about the components required for these special mitotic divisions.

The main purpose of the germ line is to produce specialized cells, sperm and oocytes, which are located at the proximal end of the gonad. Fertilization triggers completion of meiosis and a series of asymmetric and asynchronous cell divisions, which establish the *C. elegans* body plan. These embryonic divisions require the asymmetric localization of the cortical PAR-complex, which in turn governs mitotic spindle positioning and asymmetric segregation of cytoplasmic cell-fate determinants (reviewed by Cowan and Hyman, 2004). However, the molecular mechanisms underlying these events remain largely unknown.

Genetic studies in *C. elegans* have identified multiple roles for the ubiquitin system in early development, including passage through meiosis, cytoskeletal regulation and cell-fate determination (reviewed by Bowerman and Kurz, 2006). Degradation of proteins by the 26S proteasome involves the sequential action of ubiquitin (Ub)-activating (E1), Ub-conjugating (E2) and Ub-ligase (E3) enzymes that conjugate ubiquitin to the protein substrate (Hershko and Ciechanover, 1998). Members of the largest-known family of E3 ligases are assembled around cullin scaffold proteins (Petroski and Deshaies, 2005), which interact through their C-terminus with the ubiquitin-loaded E2-enzyme that provides catalytic activity. In *C. elegans* embryos, the CUL-3-based ligase regulates microtubule dynamics and spindle function at the meiosis-to-mitosis transition. Substrate recruitment is achieved by the binding of specific adaptor proteins to the amino terminus of cullins (Pintard et al., 2004; Schulman et al., 2000). CUL-3 associates with the substrate-adaptor Maternal Effect Lethal 26 (MEL-26), which is thought to bind to specific substrates by means of its Meprin and TRAF homology (MATH) domain (Pintard et al., 2003b; Xu et al., 2003). The best-characterized substrate of the CUL-3^{MEL-26} E3 ligase in *C. elegans* is the microtubule-severing protein defective meiosis 1 (MEI-1 or katanin) (Bowerman and Kurz, 2006; Kurz et al., 2002; Pintard et al., 2003b; Srayko et al., 2000). A defect in MEI-1 degradation at the meiosis-to-mitosis transition results in ectopic severing of microtubules during embryonic mitosis, which in turn leads to failures in mitotic spindle formation and in chromosome segregation (Clark-Maguire and Mains, 1994; Kurz et al., 2002; Pintard et al., 2003a). MEI-1 is a member of the large and functionally diverse family of AAA-ATPases, which use ATP hydrolysis to induce conformational changes in a wide range of substrate proteins, often leading to the inactivation of multiprotein complexes. The defining feature of the family is a structurally conserved ATPase domain that assembles into oligomeric rings and undergoes conformational changes during cycles of nucleotide binding and hydrolysis (Hanson and Whiteheart, 2005). However, despite their importance, few cellular functions and crucial substrates of AAA-ATPases have been reported.

We are interested in the regulation of cell division by ubiquitin-dependent mechanisms. In this study, we identified the conserved fidgetin-like AAA-ATPase F32D1.1 (hereafter termed FIGL-1) as a crucial component for mitotic divisions in *C. elegans*. FIGL-1 is essential in the germ line, where it might regulate microtubule function specifically in the proliferative zone. Interestingly, the CUL-3^{MEL-26} E3 ligase contributes to the spatial expression of FIGL-1 in the germ line. Our results imply that ubiquitin-dependent degradation and translational repression mechanisms might cooperate to ensure germ-line-specific expression of mitotic regulators.

Results

The AAA-ATPase FIGL-1 binds to microtubules and interacts with the substrate-adaptor MEL-26

To identify novel substrates of the CUL-3^{MEL-26} E3 ligase, we performed a yeast two-hybrid screen with MEL-26 as bait. In addition to the known MEL-26-binding proteins MEI-1 and POD-1 (Luke-Glaser et al., 2005; Pintard et al., 2003b), we found the protein FIGL-1 (Fig. 1). To confirm the two-hybrid interaction biochemically, we tested whether a hemagglutinin (HA)-tagged version of FIGL-1 expressed in *Saccharomyces cerevisiae* interacts with GST-MEL-26 produced in *Escherichia coli* by glutathione *S*-transferase (GST) pull-down assays. As shown in Fig. 1B, a fraction of HA–FIGL-1 was specifically retained on immobilized GST-MEL-26 but not on GST control beads. MEL-26 interacts with MEI-1 through its N-terminal MATH domain as mutation of a conserved cysteine to a tyrosine residue abolishes binding in vivo and in vitro (Pintard et al., 2003b; Xu et al., 2003). Like MEI-1, FIGL-1 no longer interacted with the MATH-domain mutant MEL-26-C94Y in a yeast two-hybrid assay (Fig. 1A,C), suggesting that MEL-26 uses its MATH domain to bind to FIGL-1.

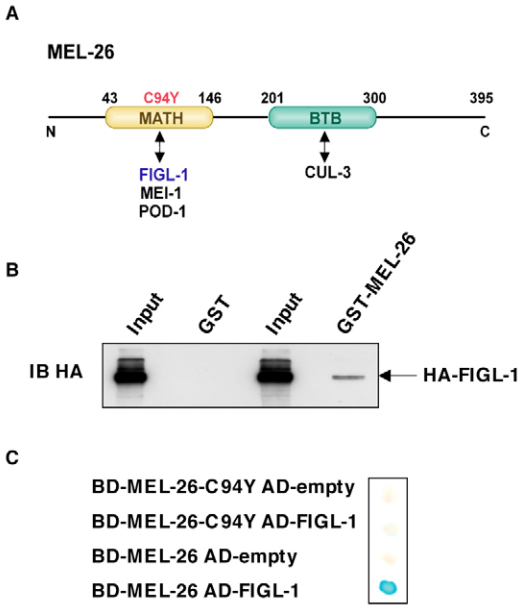

Fig. 1. MEL-26 interacts with FIGL-1 by means of the substrate-binding MATH domain. (A) The domain structure of MEL-26 and the interaction with MEI-1, POD-1 and CUL-3 are schematically indicated. The C94Y mutation lies in the MATH domain. The numbers mark the amino acids starting from the amino-terminus (N) to the carboxy-terminus (C). (B) Bacterially expressed GST-MEL-26 and, as a control, GST alone were incubated with *S. cerevisiae* extracts containing HA–FIGL-1. Bound proteins were eluted and immunoblotted with antibodies against HA. 5% of the supernatant (input) was loaded for comparison with 5% of the beads. (C) The interaction between wild-type and the C94Y mutant of MEL-26 fused to the Gal4 DNA-binding domain (BD) was characterized by two-hybrid assay with FIGL-1 fused to the Gal4 activation domain (AD). The expression of the β-galactosidase reporter was analyzed by filter assay. An empty plasmid (AD-empty) was included as a control.

Database searches and multiple sequence alignments revealed that FIGL-1 is the single *C. elegans* homolog of mammalian fidgetin (Cox et al., 2000) and fidgetin-like (Yang et al., 2005) proteins and belongs to subfamily seven of AAA-ATPases (Fig. 2) (Frickey and Lupas, 2004). Based on the amino acid sequence, fidgetin-like proteins, but not fidgetin itself, were predicted to display ATPase activity (Yakushiji et al., 2004). As F32D1.1 was previously shown to display ATPase activity in vitro (Yakushiji et al., 2004), the protein was named Fidgetin-like 1 (FIGL-1) (Yakushiji et al., 2006). FIGL-1 also

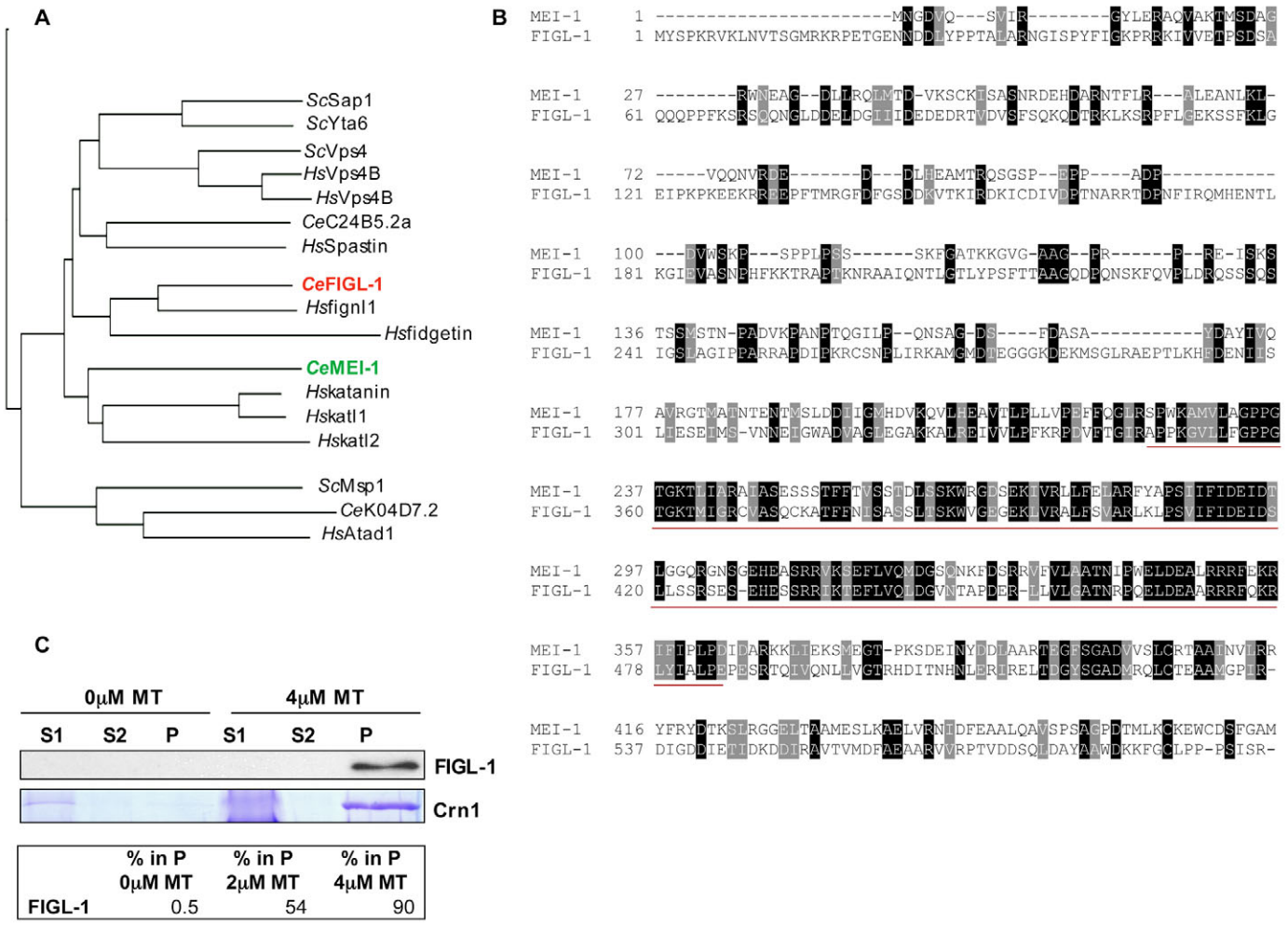

Fig. 2. FIGL-1 and MEI-1 belong to subgroup seven of the AAA-ATPases. (A) Members of subgroup seven of the AAA-ATPases are depicted in a phylogenetic tree. The closer two proteins cluster, the more recently they diverged during evolution. Whereas human and mouse contain fidgetin and fidgetin-like 1, the *C. elegans* genome only contains one gene *F32D1.1*, which was named *figl-1* and encodes Fidgetin-like 1 protein (Yakushiji et al., 2006). Species abbreviations are as follows: *Hs, Homo sapiens*; *Sc*, *S. cerevisiae*; *Ce*, *C. elegans*. (B) Alignment of MEI-1 and FIGL-1. Identical residues are shown in black and conserved substitutions on a gray background. The catalytic domain of AAA-ATPases (predicted by SMART) is underlined. Note that MEI-1 and FIGL-1 show some sequence homology outside the ATPase domain. (C) The indicated concentration (μM) of purified tubulin was polymerized in vitro, incubated with GST–FIGL-1 or yeast coronin (Crn1) as a positive control, and separated by high-speed centrifugation over a glycerol cushion. The entire pellet (P) fraction was analyzed by SDS-PAGE, whereas only 10% of the top supernatant (S1) and the bottom supernatant (S2) were loaded. The co-sedimentation of FIGL-1 with polymerized tubulin was quantified at 0 μM, 2 μM and 4 μM tubulin (n=1 for 2 μM and 4 μM tubulin, n=2 for 0 μM), and shown as a percentage (%) of the total input recovered in the pellet (bound) fraction (lower panel). In the human Cul3 negative control, only 7% (for 2 μM, n=2) and 6% (for 4 μM, n=2) of in vitro-translated Cul3 was recovered under these conditions (data not shown).

shares sequence similarity to MEI-1 on either side of its catalytic domain (Fig. 2B). To test whether FIGL-1 binds to microtubules, we performed co-sedimentation assays with purified tubulin and in vitro translated, radiolabeled FIGL-1 (Fig. 2C). As expected for subclass-seven AAA-ATPases, FIGL-1 quantitatively pelleted with polymerized tubulin, suggesting that FIGL-1 directly interacts with microtubules.

FIGL-1 is required for progression through mitosis in the transition zone of the germ line

To examine the function of FIGL-1, we inactivated *figl-1* by injecting double-stranded RNA into L3 larvae and scored embryonic lethality and sterility in the F1 progeny (Fig. 3A). Although approximately 10% of the embryos failed to hatch, the number of sterile worms in the progeny reached almost 90%. Differential interference contrast (DIC) and fluorescence microscopy revealed that these worms had greatly reduced or no germ line (Fig. 3B). Similar results were observed in the progeny of worms homozygous for a deletion allele of *figl-1(tm808)*, implying that FIGL-1 is required for the development or maintenance of the germ line. The few nuclei visible in the germ line lacking FIGL-1 all exhibited variable DNA morphologies (Fig. 3B, inset), which might have arisen from a failure in mitosis (see below). Although *figl-1(RNAi)* animals apparently lacked a germ line, they did contain distal tip cells, as visualized by expression of the *Lag-2::GFP*

transgene (Fig. 3C), implying that FIGL-1 is not required to form or maintain this stem cell. As the mitotic region is responsible for the production of germ line nuclei, our results suggest that FIGL-1 is required for cell proliferation in the germ line. Consistent with these observations, 5.6% of the F1 (*n*=287) worms depleted for *figl-1* exhibited protruding vulvas (data not shown), a phenotype characteristic of defects in progression through mitosis in somatic tissue (Furuta et al., 2000; Shakes et al., 2003). To test whether FIGL-1 is implicated in progression through mitosis, we analyzed the mitotic marker phospho-histone H3 (P-H3) by indirect immunofluorescence in *figl-1(RNAi)* animals (P0) in the mitotic zone of the germ line (Fig. 3D,E). Already 24 hours after injection, the percentage of mitotic nuclei per germ line more than doubled in *figl-1(RNAi)* compared with wild-type animals (Fig. 3D,E), indicating that FIGL-1 is required for progression through mitosis in the germ line. Taken together, we conclude that loss of *figl-1* function leads to an accumulation of mitotic nuclei in the mitotic zone.

FIGL-1 plays a non-essential role in spindle assembly or chromosome segregation during embryonic division

We next investigated whether FIGL-1 also plays a role in the mitotic progression of early *C. elegans* embryos. Indeed, indirect immunofluorescence revealed that FIGL-1 was enriched in the nucleus, although some specific cytoplasmic staining was also detectable (Fig. 4A). By contrast, MEL-26 was excluded from nuclei (Fig. 4A) (Luke-Glaser et al., 2005). However, time-lapse analysis and microtubule staining of *figl-1(RNAi)* embryos revealed no significant defects in spindle

A

figl-1(RNAi)

Time after ds RNA injection	Embryonic lethality	Sterility
0-24h (n=320)	2%	89%
24-48h (n=348)	9.3%	65%
48-62h (n=53)	3.7%	88%

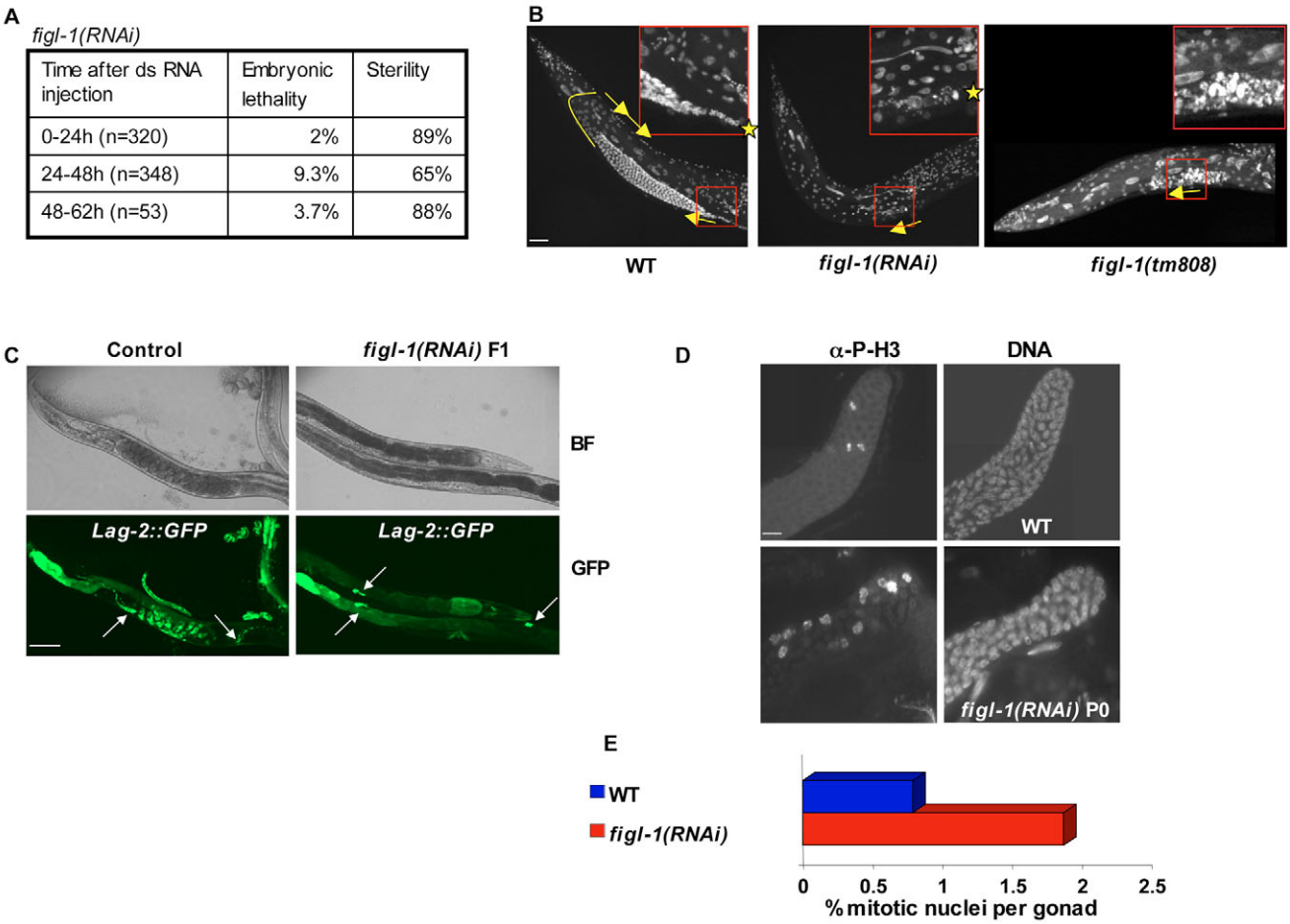

Fig. 3. FIGL-1 is required for timely mitotic progression in the germ line. (A) L3 larvae were injected with *figl-1* dsRNA and the resulting embryonic lethality and sterility of their F1 progeny was quantified and expressed as a percentage (%) of the total number (*n*) of progeny analyzed. Although the embryonic lethality is low, the percentage of sterile progeny reaches 89%. (B) The gonadal arms at the tail end of wild-type (left image), *figl-1(RNAi)*-depleted progeny and *figl-1(tm808)*-homozygous animals (right image) were visualized within the worm by Hoechst staining. The stars mark the start of the 'mitotic gonad' in the *figl-1(RNAi)* progeny, and the arrows indicate the mitotic and meiotic progression in the U-shaped gonad. The few nuclei that were left in the *figl-1(RNAi)* and *figl-1(tm808)* progeny all display abnormal sizes and structures (insets). Bar, 10 μm. (C) *figl-1(RNAi)* animals express the distal-tip cell marker *Lag2::GFP*. GFP expressed by a *Lag-2::GFP* transgene (arrows) is visualized with a fluorescent microscope in control (bottom left) or *figl-1(RNAi)* animals (bottom right). Upper panels show animals visualized by bright-field microscopy. Bar, 100 μm. (D,E) The number of mitotic nuclei was determined in gonads of wild-type (WT) and *figl-1(RNAi)* animals by immunofluorescence with antibodies against phosphorylated histone H3 (D, left images). The DNA was visualized by Hoechst staining (D, right images). The result was quantified and plotted as a percentage (%) of mitotic cells per gonad (E). Note that the number of nuclei with a positive phospho-H3 signal is higher in *figl-1(RNAi)* animals ($P=1.17\times10^{-7}$).

formation and chromosome segregation (data not shown), suggesting that FIGL-1 is not required for mitotic progression at the one-cell stage. Minor defects in spindle function and chromosome segregation are exacerbated by the absence of functional mitotic checkpoints, which delay the cell cycle and thus allow more time to achieve correct attachment of replicated DNA to the spindle apparatus (Gardner and Burke, 2000). To test whether functional mitotic checkpoints might be required to rescue *figl-1(RNAi)* embryos, we monitored lethality after 24 and 48 hours in embryos simultaneously inactivated for *figl-1* and a conserved component of the mitotic spindle-assembly and chromosome-attachment checkpoints (Fig. 4B,C). *Y54G9A.6* encodes a homolog of *S. cerevisiae* Bub3p (Oegema and Hyman, 2006), whereas *mdf-1* and *san-1* encode the homologs of *S. cerevisiae* Mad1p and Mad3p, respectively (Kitagawa and Rose, 1999; Nystul et al., 2003). Whereas depletion of these checkpoint proteins alone showed no embryonic lethality, 19-27% (24 and 48 hours after injection, respectively) of *san-1(RNAi); figl-1(RNAi)* and up to 57% of the *Y54G9A.6(RNAi); figl-1(RNAi)* double-depleted embryos did not survive (Fig. 4B,C). The most dramatic synthetic-lethal effect was observed upon co-depletion of *figl-1* and *mdf-1*, which resulted in 73% of the embryos failing to hatch. We thus conclude that embryos lacking FIGL-1 require a functional mitotic checkpoint for survival.

FIGL-1 is expressed around chromosomes in mitotic germ cells, and its levels and expression pattern in the germ line is dependent on CUL-3^{MEL-26} activity

To characterize the relationship between FIGL-1 and MEL-26 in vivo, we next compared their spatial patterns of expression in the *C. elegans* germ line. Interestingly, indirect immunofluorescence using affinity-purified antibodies revealed that FIGL-1 was predominantly expressed around chromosomes in nuclei of cells in the mitotic zone of the germ line (Fig. 5A, and inset). Quantification of these results revealed that FIGL-1 levels in the mitotic zone were twofold higher compared with its expression in meiotic cells (Fig. 5A,C). By contrast, MEI-1 expression was uniform in the germ line and restricted neither to the meiotic nor the mitotic zone. Moreover, MEI-1 was absent from chromatin (data not shown), indicating that MEI-1 and FIGL-1 might disassemble protein complexes in different cellular compartments. Interestingly, low levels of MEL-26 were detected in the mitotic zone, but MEL-26 was prominently expressed and present on chromosomes during meiotic stages (Fig. 5A). The transition

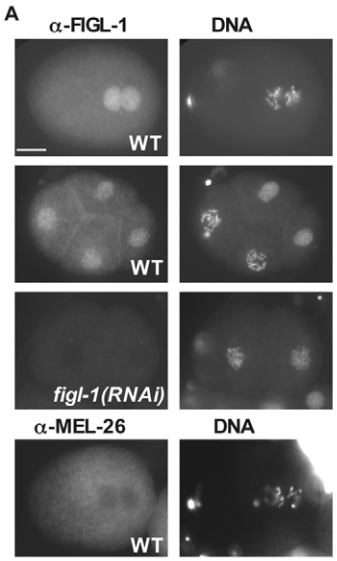

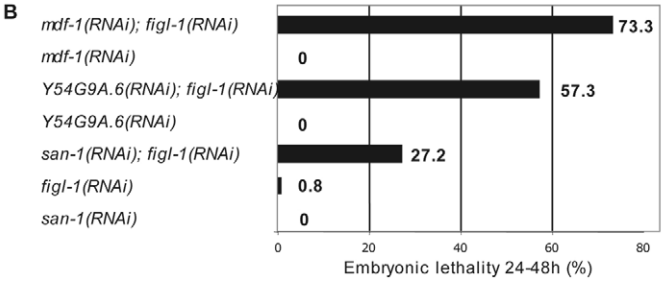

C

Genotype	Number of L3 larvae injected	Embryonic Lethality (0-24h)	Embryonic Lethality (24-48h)
mdf-1(RNAi); figl-1(RNAi)	5	0% n = 14	**73.3%** n = 101
mdf-1(RNAi)	3	0% n = 9	0% n = 143
Y54G9A.6(RNAi; figl-1(RNAi)	7	33.3% n=78	**57.3%** n=347
Y54G9A.6(RNAi)	8	10.9% n=108	0% n=343
san-1(RNAi); figl-1(RNAi)	10	18.8% n=101	**27.2%** n=357
figl-1(RNAi)	13	0% n=220	0.8% n=628
san-1(RNAi)	6	0% n=56	0% n=240

n = number of embryos

Fig. 4. FIGL-1 activity is vital for *C. elegans* embryos in the absence of a functional spindle-assembly checkpoint. (A) The localization of FIGL-1 and MEL-26 was determined by immunofluorescence with affinity-purified antibodies in wild-type and *figl-1(RNAi)* early embryos. The DNA was visualized by Hoechst staining (right panels). Bar, 10 μm. (B,C) L3 larvae were injected with double-stranded RNA against *figl-1* or the mitotic checkpoint components *san-1* (*S. cerevisiae MAD3*), *mdf-1* (*S. cerevisiae MAD1*) or *Y54G9A.6* (*S. cerevisiae BUB3*) either alone or in combination. Embryonic lethality was scored after the times indicated and plotted (24-48 hours). The values obtained after 24 and 48 hours of inactivation are listed in panel C, and schematically presented in panel B.

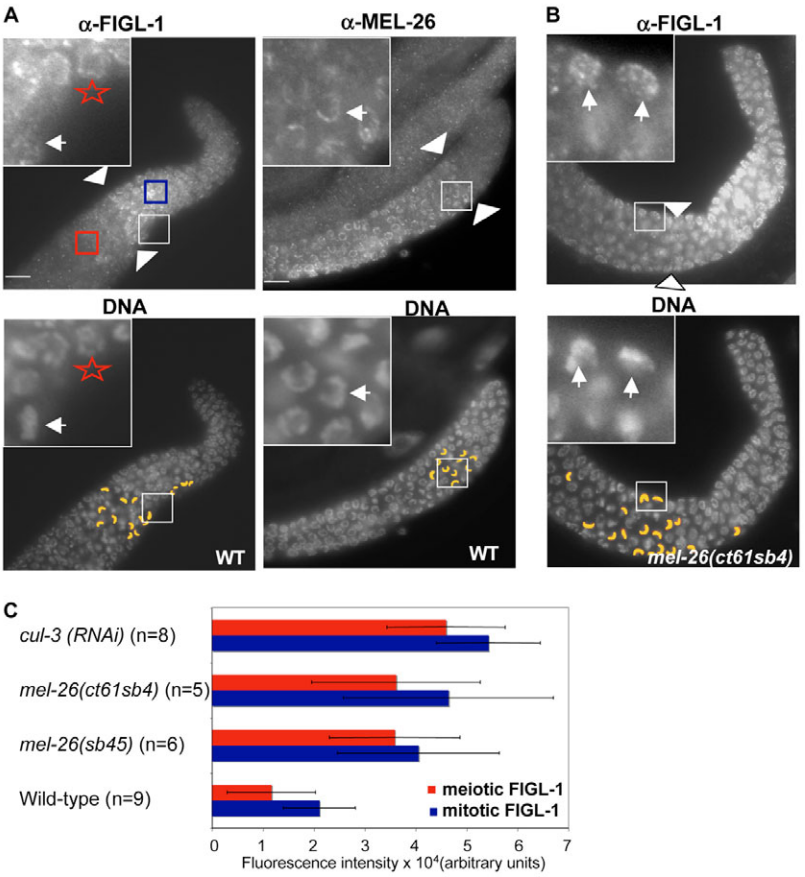

Fig. 5. FIGL-1 is expressed in the mitotic zone of the germ line and accumulates in *mel-26* mutants or *cul-3*-depleted animals. (A) The localization of FIGL-1 and MEL-26 was determined by immunofluorescence in the gonads of wild-type animals by using affinity-purified antibodies against FIGL-1 (top left) and MEL-26 (top right). The DNA was visualized by Hoechst staining (bottom row). The beginning of meiosis (transition zone) is marked by arrowheads and is defined as the region where 60% of the nuclei are in meiotic prophase, as indicated by the crescent-shaped nuclei (depicted in yellow). The white box delineates the area shown at higher magnification in the inset. Stars mark nuclei before meiotic prophase; the short arrows in insets point to crescent-shaped nuclei in meiotic prophase. Note that the staining of FIGL-1 is significantly reduced ($P<0.05$) in cells entering into meiosis compared with cells in mitosis. Bars, 10 μm. (B) The expression of FIGL-1 (top panel) was investigated by immunofluorescence as described for panel B in gonads of *mel-26(ct61sb4)* animals. All stainings were performed under the same conditions to allow comparison. The DNA was visualized by Hoechst staining (bottom panel). The inset shows a higher magnification of the boxed area. (C) The fluorescence intensity of FIGL-1 staining in a set area in the mitotic (blue) and meiotic (red) zone of multiple wild-type, *mel-26(sb45)*, *mel-26(ct61sb4)* and *cul-3(RNAi)* gonads was quantified as described above (see Materials and Methods) and shown in a bar diagram along with standard deviations. Note that FIGL-1 accumulates in gonads of worms that are defective for CUL-3^{MEL-26} function, and its expression extends into the meiotic zone.

zone from mitosis to meiosis starts where 60% of the nuclei show the crescent-shaped morphology (colored yellow) that is a hallmark of early meiotic prophase (Eckmann et al., 2004; Kimble and Crittenden, 2005; MacQueen and Villeneuve, 2001). Therefore, MEL-26 and FIGL-1 exhibit a seemingly complementary localization within the germ line of wild-type animals – a relationship expected for a substrate and its specific adaptor for degradation. The border of their respective localizations seems to correlate with the transition zone, which separates the mitotic from the meiotic cells (or nuclei).

To investigate whether CUL-3^{MEL-26} activity was required to regulate and restrict FIGL-1 expression to the mitotic zone, we analyzed FIGL-1 expression in the germ line of *mel-26(sb45)* animals, which harbor the C94Y mutation that abolishes its binding to FIGL-1 (Fig. 1), and *mel-26(ct61sb4)* animals, which are considered to be bone fide null mutants (Dow and Mains, 1998). Interestingly, in contrast to wild-type animals, FIGL-1 expression was readily detected in germ cells of *mel-26(sb45)* and *mel-26(ct61sb4)* mutant animals that, based on nuclear morphology, have entered meiotic prophase (Fig. 5B,C, insets; and data not shown). Similar results were also obtained in gonads prepared from *cul-3(RNAi)* animals (data not shown), suggesting that CUL-3^{MEL-26} activity is required for FIGL-1 degradation at the mitosis-to-meiosis transition in the germ line. Nevertheless, FIGL-1 levels decreased at later meiotic stages, indicating that the ubiquitin system might not be the only mechanism to downregulate FIGL-1 levels during meiosis. Alternatively, another ligase might account for FIGL-1 degradation. Surprisingly, although MEL-26 expression is low, FIGL-1 accumulated at least twofold in the mitotic zone of the germ line of *mel-26(sb45)* and *mel-26(ct61sb4)* mutant animals (Fig. 5C). This result implies that CUL-3^{MEL-26} activity not only prevents accumulation of FIGL-1 during meiosis but might also regulate FIGL-1 levels during the mitotic divisions in the germ line.

Discussion

FIGL-1 regulates mitosis in the germ line and early embryos, most likely by affecting the microtubule cytoskeleton

Our results suggest that FIGL-1, the sole *C. elegans* homolog of the mammalian fidgetin and fidgetin-like proteins (Fig. 2), is implicated in the regulation of chromosome segregation during mitosis of germ line and somatic cells. By analogy to other AAA-ATPases, fidgetin-like proteins are predicted to use the energy released from ATP hydrolysis to disrupt multisubunit complexes. Although further work is required to identify the molecular target(s), several lines of evidence suggest that FIGL-1 affects microtubule stability. Like the microtubule-severing proteins spastin (Trotta et al., 2004) and katanin (Hartman and Vale, 1999; McNally and Vale, 1993), FIGL-1 belongs to the same subfamily seven of AAA-ATPases and displays ATPase activity in vitro (Yakushiji et al., 2004). Moreover, purified FIGL-1 binds strongly to microtubules in co-pelleting assays (Fig. 2C) and associates with chromosomes in the germ line (Fig. 5A). The mitotic defects reflected by the accumulation of mitotic nuclei in *figl-1(RNAi)* in the gonad might result from increased microtubule stability as dynamic microtubules are a

prerequisite for assembly and function of the mitotic spindle. After breakdown of the nuclear envelope, astral microtubules must capture chromosomes and align them on the mitotic spindle. During this process, chromosomes play an active role by nucleating microtubules in their immediate vicinity (Tulu et al., 2003). However, microtubule nucleation by chromosomes is inefficient, and it is believed that microtubule severing might be required to locally generate more microtubule ends. For example, the microtubule-severing activity of MEI-1 is essential for the assembly of the meiotic spindle in *C. elegans*. We thus speculate that FIGL-1 regulates chromosomes congression and/or segregation by severing microtubules in the vicinity of mitotic chromosomes (Srayko et al., 2006). Indeed, chromosomes actively depolymerize microtubules at their plus-end while being reeled towards spindle poles by minus-end depolymerization. However, the activities controlling these processes are still poorly understood. Interestingly, a recent study revealed that *Drosophila* Fidgetin, together with Spastin, regulates chromosome segregation by promoting minus-end microtubule depolymerization at the centrosome-associated γ-tubulin ring complex (Zhang et al., 2007). Indeed, RNAi depletion of Fidgetin in S2 cells dramatically reduced microtubule flux, thereby compromising anaphase A. We thus propose that FIGL-1 might similarly use its microtubule-severing activity to regulate mitotic spindle function and chromosome segregation in germ-line nuclei during early larvae stages, resulting in the observed germ-line-less phenotype. Why FIGL-1 function is essential in the germ line, whereas its loss creates defects that can be rescued by the spindle checkpoint in early embryos remains to be investigated. Moreover, it will be interesting to determine whether Spastin collaborates with FIGL-1 and contributes to this process in both the *C. elegans* germ line and early embryos.

FIGL-1 might be a novel substrate of the CUL-3^{MEL-26} ligase in vivo

Our results imply that the CUL-3^{MEL-26} ligase regulates FIGL-1 levels in the mitotic zone of the germ line and contributes to restrict FIGL-1 expression to this region by targeting its degradation in the transition zone. It is thus possible that loss and gain of *figl-1* function might alter progression through mitosis. Accumulation of FIGL-1 in the gonad could lead to decreased stability of microtubules and interfere with mitotic and/or meiotic progression by causing chromosome attachment and segregation problems. Indeed, it has been shown that injection of the microtubule-destabilizing drug nocodazole triggers an increase of mitotic nuclei in the gonad (Kitagawa and Rose, 1999). Thus, the CUL-3^{MEL-26} ligase could be important to temporally and spatially regulate FIGL-1 levels in the germ line.

Several mitotic regulators have previously been localized to the mitotic zone of the gonad, whereas meiotic regulators are restricted to the meiotic zone (Kimble and Crittenden, 2005). Spatial restriction of these regulators has been reported to be governed by translational control. To our knowledge, this is the first experimental evidence that ubiquitin-dependent degradation contributes to this expression pattern in the *C. elegans* germ line. Whereas the CUL-3^{MEL-26} complex triggers FIGL-1 degradation during mitosis and meiosis in the gonadal syncitium, MEI-1 is stable in oocytes and on the meiotic spindle in early embryos (Fig. 6). Conversely, MEI-1 is degraded at the meiosis-to-mitosis transition, whereas FIGL-1 is stable in nuclei of early embryos, where it contributes to the mitotic divisions. A mutation within the MEL-26 MATH domain abolishes binding to both MEI-1 and FIGL-1, indicating that MEL-26 uses the same interface to bind to both substrates. These results imply that additional regulators must act at the level of the substrates to trigger their recognition by the ligase. Indeed, phosphorylation of MEI-1 by Minibrain Kinase 2 (MBK-2) contributes to MEI-1 degradation in vivo (Pellettieri et al., 2003; Stitzel et al., 2006). Furthermore, bacterially expressed (and therefore non-phosphorylated) FIGL-1 or MEI-1 only interact weakly with purified MEL-26 in vitro (our unpublished data). The MBK-2 phosphorylation sites are not conserved in FIGL-1, implying that differential phosphorylation might be capable of specifically targeting MEI-1 in early embryos. Alternatively, the distinct subcellular localization of MEL-26 and FIGL-1 in early embryos might also contribute to its stabilization. Interestingly, whereas MEL-26 and FIGL-1 both accumulate around chromosomes in the overlapping zone of the gonad, MEL-26 is predominantly cytoplasmic after fertilization. Nuclear FIGL-1 might thus be protected from degradation at this stage of development, whereas cytoplasmic MEI-1 might be readily ubiquitinylated by the CUL-3^{MEL-26} E3 ligase. Clearly, further work will be required to distinguish these and other mechanisms.

Taken together, the available evidence suggest that, at least in *C. elegans*, the two AAA-ATPases MEI-1 and FIGL-1 are physiological targets of the CUL-3^{MEL-26} E3 ligase (Fig. 6). It is thus tempting to speculate that other AAA-ATPases might

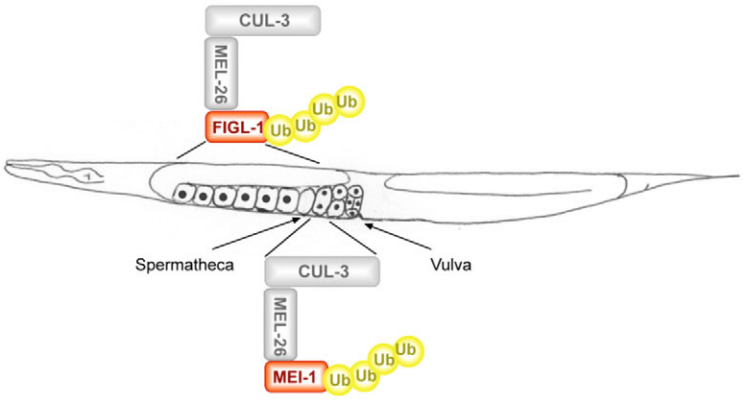

Fig. 6. The CUL-3^{MEL-26} ubiquitin ligase might target two distinct AAA-ATPases for degradation at different developmental stages. The CUL-3^{MEL-26} complex degrades FIGL-1 during meiotic stages in the gonad. By contrast, FIGL-1 is largely protected from degradation in the mitotic zone, possibly because of spatial restriction of MEL-26. At the meiosis-to-mitosis transition, the same E3 ligase targets MEI-1 for degradation (Pintard et al., 2003b). The different timing of degradation of FIGL-1 and MEI-1 might be regulated by phosphorylation by means of kinases present at these different developmental stages.

similarly be regulated by ubiquitin-dependent degradation, perhaps by Cul3- or BTB-based ligases. In neurons, the BTB-protein gigaxonin controls the degradation of microtubule-regulating proteins (Allen et al., 2005; Wang et al., 2005). Moreover, HeLa cells depleted for hCUL3 by RNAi exhibit defects in microtubule dynamics (Sumara et al., 2007), suggesting that hCUL3-based E3 ligases control the activity of several microtubule-regulating proteins in human cells. Finally, MEI-1 and FIGL-1 are highly conserved (Fig. 2) and their function might thus also be important in mammalian cells. Indeed, a mouse fidgetin mutant was previously discovered in 1943 and displays pleiotropic phenotypes, including head-shaking, small eyes and skeletal defects (Gruneberg, 1943). Although the molecular basis of these phenotypes has not been resolved, it is tempting to speculate that some of them might be caused by defects in microtubule function and cell division.

Materials and Methods

Database searches and bioinformatics

We used pBLAST (NCBI) to search for amino acid sequence homologies, ClustalW (EMBnet: www.ch.embnet.org) for protein sequence alignments and Boxshade (EMBnet) for presenting sequence alignments. The locations of the AAA-ATPase domains in MEI-1 and FIGL-1 were determined by SMART (EMBL: smart.embl-heidelberg.de). The phylogenetic tree was based on a multiple sequence alignment generated by ClustalW and was designed by the 'neighbor joining' algorithm. Accession numbers of the proteins used to generate the phylogenetic tree are the following: *S. cerevisiae*: Sap1: NP_010966; Yta6: NP_015251; Vps4: NP_015499; Msp1: NP_011542; *Homo sapiens*: Vps4A: NP_037377; Vps4B: NP_004860; Spastin: Q9UBPO; Fignl1: NP_071399; katanin: 075449; Katl1: Q9BW62; Katl2: NP_112593; Atad1: AAH63530; *C. elegans*: C24B5.2a: NP_741586; FIGL-1: NP_504197; MEI-1: P34808; K04D7.2: CAC42312.

Native yeast extracts and GST pull-down

GST-MEL-26 was expressed in bacteria, as reported previously (Pintard et al., 2003a). HA–FIGL-1 was expressed in *S. cerevisiae* from the plasmid pACT2-HA (Clontech). Yeast native extracts were obtained by breaking the cells for 15 minutes at 4°C with glass beads in 50 mM Tris-HCl (pH 7.5), 150 mM NaCl, 5 mM $MgCl_2$, NP-40 (1:500, from Fluka), complete EDTA-free protease inhibitors (Roche), 1 mM PMSF (Fluka), 2 μg/ml leupeptin (Calbiochem) and 20 μg/ml DNAse. Glutathione beads (Amersham Biosciences) and GST or GST-MEL-26 were incubated for 45 minutes at room temperature and washed with the aforementioned buffer. 1 mg of total yeast extract was added to GST and GST-MEL-26 coupled to 100 μl beads, respectively, and incubated for 1.5 hours at 4°C. After washing, equal amounts (5%) of the input and the bead fractions were analyzed by SDS-PAGE and western blotting (anti-HA).

Antibody production and immunoblotting

Antibodies against the following peptides and proteins were used in this study: HA-11 (Babco), α-tubulin (Sigma), phospho-histone 3 (Upstate); MEL-26 (Pintard et al., 2003b) and FIGL-1 (this study). FIGL-1 polyclonal antibodies were raised against an N-terminal fragment (amino acids 1-333) of bacterially produced GST–FIGL-1, as described previously (Pintard et al., 2003a). For immunocytochemistry, the antibodies were purified on GST–FIGL-1 bound to nitrocellulose strips.

Immunocytochemistry and microscopy

Animals expressing the *lag-2::GFP* transgene were paralyzed with 0.2 mM levamisole (Sigma), mounted on agarose pads and visualized under a fluorescent stereomicroscope. The gonads were dissected by opening the worms in M9 buffer behind the pharyngeal bulb. Worms and embryos were freeze-cracked by flipping off the coverslip, immobilized on poly-lysine-coated slides and fixed for 20 minutes in methanol at room temperature. Temperature-sensitive alleles were shifted for 24 hours to the restrictive temperature before staining. Affinity-purified anti–FIGL-1 antibody was used at a dilution of 1:250. Secondary antibodies were purchased from Molecular Probes. DNA was stained by Hoechst (Sigma). Microscopy was carried out with a Zeiss Axiovert 200M equipped with DIC optics and a Hamamatsu camera. Image J was used to quantify the immunofluorescence stainings. Equal areas of the mitotic and the meiotic zone were measured and the slide background was subtracted. Nine gonads were analyzed for wild-type, eight for *cul-3(RNAi)*, six for *mel-26(sb45)* and five for *mel-26(sb4)* (data not shown). Gonads of each genotype were prepared, stained and processed in parallel and under the same conditions to allow for comparison.

C. elegans strains and manipulations

The *C. elegans* isolate N2 Bristol was used as wild-type, and all manipulations followed standard conditions (Brenner, 1974). The following strains were studied during this work: *mel-26(or543)*, *mel-26(or184)*, *mel-26(ct61sb4)*, JK2868 [*qIs56* (IV or V); *lag-2::GFP*] (Blelloch et al., 1999), GFP::histone H2B *(his-11)*; GFP::β-tubulin *(tbb-2)* {available from the *Caenorhabditis* Genetics Center http://biosci.umn.edu/CGC/CGChomepage.htm as 'TY3558' *unc-119(ed3) ruIs32[pie-1::GFP::his-11] III; ojIs1[tbb-2::GFP]*} and *figl-1(tm808)*. The deletion in *figl-1(tm808)* starts in the first exon at base-pair 369 and ends at base-pair 731 in the second exon, thus allowing the expression of a 47-residue peptide instead of the 160-residue FIGL-1 open reading frame.

RNA-mediated interference (RNAi)

RNAi was performed by injecting *figl-1* or *cul-3* double-stranded (ds) RNA into L3 larvae or young adults, or by feeding L1 larvae on NGM plates containing 3 mM IPTG. The construct to generate *cul-3* dsRNA was described previously (Pintard et al., 2003a). *figl-1* dsRNA was generated by amplifying the third exon. The constructs targeting *san-1*, *mdf-1* and *Y54G9A.6* originate from the feeding library of the laboratory of J. Ahringer (The Wellcome Trust/Cancer Research UK Gurdon Institute, Cambridge, UK) and were confirmed by sequencing the inserts.

Statistical analysis

The probability that two data sets originate from the same distribution was tested with a Student's *t*-test, allowing two-tailed distribution and unequal variances.

Yeast transformations, manipulations and two-hybrid screen

Yeast Y190 (Clontech) cells were transformed by the lithium acetate method and handled following standard protocols (Guthrie and Fink, 1991). The yeast two-hybrid screen and the LacZ assays were performed as described previously (Luke-Glaser et al., 2005).

Microtubule and co-pelleting assays in vitro

Microtubule co-pelleting assays with taxol-stabilized microtubules were prepared as described previously (Hyman et al., 1991), with GST–FIGL-1 produced in *E. coli*. Purified *S. cerevisiae* Crn1 was a gift from Bruce Goode (Brandeis University, Waltham, MA). FIGL-1 and Crn1 were incubated with microtubules for 20 minutes at 37°C and spun down for 10 minutes over a 50% glycerol cushion (200 μl) at 135,000 ***g*** in a TLA 100.3 rotor. Although the whole pellet was analyzed by SDS-PAGE, only 10% of the supernatants (cushion) were loaded. The quantification of retained proteins was carried out by ImageJ. In vitro translated human Cul3 and Miz1 were used as negative controls (data not shown).

We are grateful to B. Goode for purified yeast Crn1, B. Bowerman for the GFP::histone H2B; GFP::β-tubulin strain, the laboratory of Shohei Mitani for the *C. elegans* deletion mutant *tm808*, J. Kimble for the strain expressing the *lag-2::GFP* transgene *(JK2868)* and the laboratory of J. Ahringer for feeding vectors. We thank K. Hofmann for kindly providing the phylogenetic tree of the meiotic AAA-ATPase subfamily and C. Rupp for technical support. We are grateful to B. Luke, S. Leidel, M. Gotta, P. Gönczy and T. Kurz for critical reading of the manuscript, and members of the M.P., M.T. and M. Gotta laboratories for helpful discussion. L.P. was supported by a traveling fellowship from the *Journal of Cell Science*, and an ATIP grant from the CNRS. The research of S.L.-G. was financed by a fellowship from the Boehringer Ingelheim Fonds. The laboratory of M.P. was supported by grants from the SNF and the ETHZ.

References

Allen, E., Ding, J., Wang, W., Pramanik, S., Chou, J., Yau, V. and Yang, Y. (2005). Gigaxonin-controlled degradation of MAP1B light chain is critical to neuronal survival. *Nature* **438**, 224-228.

Blelloch, R., Anna-Arriola, S. S., Gao, D., Li, Y., Hodgkin, J. and Kimble, J. (1999). The gon-1 gene is required for gonadal morphogenesis in Caenorhabditis elegans. *Dev. Biol.* **216**, 382-393.

Bowerman, B. and Kurz, T. (2006). Degrade to create: developmental requirements for ubiquitin-mediated proteolysis during early C. elegans embryogenesis. *Development* **133**, 773-784.

Brenner, S. (1974). The genetics of *Caenorhabditis elegans*. *Genetics* **77**, 71-94.

Champion, M. D. and Hawley, R. S. (2002). Playing for half the deck: the molecular biology of meiosis. *Nat. Cell Biol.* **4**, s50-s56.

Clark-Maguire, S. and Mains, P. E. (1994). Localization of the mei-1 gene product of Caenorhabditis elegans, a meiotic-specific spindle component. *J. Cell Biol.* **126**, 199-209.

Cowan, C. R. and Hyman, A. A. (2004). Asymmetric cell division in C. elegans: cortical polarity and spindle positioning. *Annu. Rev. Cell Dev. Biol.* **20**, 427-453.

Cox, G. A., Mahaffey, C. L., Nystuen, A., Letts, V. A. and Frankel, W. N. (2000). The

mouse fidgetin gene defines a new role for AAA family proteins in mammalian development. *Nat. Genet.* **26**, 198-202.
Dow, M. R. and Mains, P. E. (1998). Genetic and molecular characterization of the *Caenorhabditis elegans* gene, *mel-26*, a postmeiotic negative regulator of mei-1, a meiotic-specific spindle component. *Genetics* **150**, 119-128.
Eckmann, C. R., Crittenden, S. L., Suh, N. and Kimble, J. (2004). GLD-3 and control of the mitosis/meiosis decision in the germline of Caenorhabditis elegans. *Genetics* **168**, 147-160.
Frickey, T. and Lupas, A. N. (2004). Phylogenetic analysis of AAA proteins. *J. Struct. Biol.* **146**, 2-10.
Furuta, T., Tuck, S., Kirchner, J., Koch, B., Auty, R., Kitagawa, R., Rose, A. M. and Greenstein, D. (2000). EMB-30: an APC4 homologue required for metaphase-to-anaphase transitions during meiosis and mitosis in *Caenorhabditis elegans*. *Mol. Biol. Cell* **11**, 1401-1419.
Gardner, R. D. and Burke, D. J. (2000). The spindle checkpoint: two transitions, two pathways. *Trends Cell Biol.* **10**, 154-158.
Gruneberg, H. (1943). Two new mutant genes in the house mouse. *J. Genet.* **45**, 22-28.
Guthrie, C. and Fink, G. R. (1991). Guide to yeast genetics and molecular biology. *Methods Enzymol.* **194**, 1-863.
Hanson, P. I. and Whiteheart, S. W. (2005). AAA+ proteins: have engine, will work. *Nat. Rev. Mol. Cell Biol.* **6**, 519-529.
Hartman, J. J. and Vale, R. D. (1999). Microtubule disassembly by ATP-dependent oligomerization of the AAA enzyme katanin. *Science* **286**, 782-785.
Hershko, A. and Ciechanover, A. (1998). The ubiquitin system. *Annu. Rev. Biochem.* **67**, 425-479.
Hyman, A., Drechsel, D., Kellogg, D., Salser, S., Sawin, K., Steffen, P., Wordeman, L. and Mitchison, T. (1991). Preparation of modified tubulins. *Methods Enzymol.* **196**, 478-485.
Kimble, J. E. and White, J. G. (1981). On the control of germ cell development in *Caenorhabditis elegans*. *Dev. Biol.* **81**, 208-219.
Kimble, J. E. and Crittenden, S. L. (2005). Germline proliferation and its control. In *Wormbook* (ed. The *C. elegans* Research Community), doi:10.1895/wormbook.1.13.1.
Kitagawa, R. and Rose, A. M. (1999). Components of the spindle-assembly checkpoint are essential in *Caenorhabditis elegans*. *Nat. Cell Biol.* **1**, 514-521.
Kurz, T., Pintard, L., Willis, J. H., Hamill, D. R., Gonczy, P., Peter, M. and Bowerman, B. (2002). Cytoskeletal regulation by the Nedd8 ubiquitin-like protein modification pathway. *Science* **295**, 1294-1298.
Luke-Glaser, S., Pintard, L., Lu, C., Mains, P. E. and Peter, M. (2005). The BTB protein MEL-26 promotes cytokinesis in *C. elegans* by a CUL-3-independent mechanism. *Curr. Biol.* **15**, 1605-1615.
MacQueen, A. J. and Villeneuve, A. M. (2001). Nuclear reorganization and homologous chromosome pairing during meiotic prophase require C. elegans chk-2. *Genes Dev.* **15**, 1674-1687.
Marston, A. L. and Amon, A. (2004). Meiosis: cell-cycle controls shuffle and deal. *Nat. Rev. Mol. Cell Biol.* **5**, 983-997.
McNally, F. J. and Vale, R. D. (1993). Identification of katanin, an ATPase that severs and disassembles stable microtubules. *Cell* **75**, 419-429.
Nakayama, K. I. and Nakayama, K. (2006). Ubiquitin ligases: cell-cycle control and cancer. *Nat. Rev. Cancer* **6**, 369-381.
Nystul, T. G., Goldmark, J. P., Padilla, P. A. and Roth, M. B. (2003). Suspended animation in *C. elegans* requires the spindle checkpoint. *Science* **302**, 1038-1041.
Oegema, K. and Hyman, A. A. (2006). Cell division. In *Wormbook* (ed. The *C. elegans* Research Community), doi:10.1895/wormbook.1.72.1.
Pellettieri, J., Reinke, V., Kim, S. K. and Seydoux, G. (2003). Coordinate activation of maternal protein degradation during the egg-to-embryo transition in *C. elegans*. *Dev. Cell* **5**, 451-462.
Petroski, M. D. and Deshaies, R. J. (2005). Function and regulation of cullin-RING ubiquitin ligases. *Nat. Rev. Mol. Cell Biol.* **6**, 9-20.
Pintard, L., Kurz, T., Glaser, S., Willis, J. H., Peter, M. and Bowerman, B. (2003a). Neddylation and deneddylation of CUL-3 is required to target MEI-1/Katanin for degradation at the meiosis-to-mitosis transition in *C. elegans*. *Curr. Biol.* **13**, 911-921.
Pintard, L., Willis, J. H., Willems, A., Johnson, J. L., Srayko, M., Kurz, T., Glaser, S., Mains, P. E., Tyers, M., Bowerman, B. et al. (2003b). The BTB protein MEL-26 is a substrate-specific adaptor of the CUL-3 ubiquitin-ligase. *Nature* **425**, 311-316.
Pintard, L., Willems, A. and Peter, M. (2004). Cullin-based ubiquitin ligases: Cul3-BTB complexes join the family. *EMBO J.* **23**, 1681-1687.
Schulman, B. A., Carrano, A. C., Jeffrey, P. D., Bowen, Z., Kinnucan, E. R., Finnin, M. S., Elledge, S. J., Harper, J. W., Pagano, M. and Pavletich, N. P. (2000). Insights into SCF ubiquitin ligases from the structure of the Skp1-Skp2 complex. *Nature* **408**, 381-386.
Shakes, D. C., Sadler, P. L., Schumacher, J. M., Abdolrasulnia, M. and Golden, A. (2003). Developmental defects observed in hypomorphic anaphase-promoting complex mutants are linked to cell cycle abnormalities. *Development* **130**, 1605-1620.
Srayko, M., Buster, D. W., Bazirgan, O. A., McNally, F. J. and Mains, P. E. (2000). MEI-1/MEI-2 katanin-like microtubule severing activity is required for *Caenorhabditis elegans* meiosis. *Genes Dev.* **14**, 1072-1084.
Srayko, M., O'Toole, E. T., Hyman, A. A. and Muller-Reichert, T. (2006). Katanin disrupts the microtubule lattice and increases polymer number in C. elegans meiosis. *Curr. Biol.* **16**, 1944-1949.
Stitzel, M. L., Pellettieri, J. and Seydoux, G. (2006). The C. elegans DYRK kinase MBK-2 marks oocyte proteins for degradation in response to meiotic maturation. *Curr. Biol.* **16**, 56-62.
Sumara, I., Quadroni, M., Frei, C., Olma, M. H., Sumara, G., Ricci, R. and Peter, M. (2007). A cul3-based E3 ligase removes aurora B from mitotic chromosomes, regulating mitotic progression and completion of cytokinesis in human cells. *Dev. Cell* **12**, 887-900.
Trotta, N., Orso, G., Rossetto, M. G., Daga, A. and Broadie, K. (2004). The hereditary spastic paraplegia gene, spastin, regulates microtubule stability to modulate synaptic structure and function. *Curr. Biol.* **14**, 1135-1147.
Tulu, U. S., Rusan, N. M. and Wadsworth, P. (2003). Peripheral, non-centrosome-associated microtubules contribute to spindle formation in centrosome-containing cells. *Curr. Biol.* **13**, 1894-1899.
Wang, W., Ding, J., Allen, E., Zhu, P., Zhang, L., Vogel, H. and Yang, Y. (2005). Gigaxonin interacts with tubulin folding cofactor B and controls its degradation through the ubiquitin-proteasome pathway. *Curr. Biol.* **15**, 2050-2055.
Xu, L., Wei, Y., Reboul, J., Vaglio, P., Shin, T. H., Vidal, M., Elledge, S. J. and Harper, J. W. (2003). BTB proteins are substrate-specific adaptors in an SCF-like modular ubiquitin ligase containing CUL-3. *Nature* **425**, 316-321.
Yakushiji, Y., Yamanaka, K. and Ogura, T. (2004). Identification of a cysteine residue important for the ATPase activity of *C. elegans* fidgetin homologue. *FEBS Lett.* **578**, 191-197.
Yakushiji, Y., Nishikori, S., Yamanaka, K. and Ogura, T. (2006). Mutational analysis of the functional motifs in the ATPase domain of Caenorhabditis elegans fidgetin homologue FIGL-1: firm evidence for an intersubunit catalysis mechanism of ATP hydrolysis by AAA ATPases. *J. Struct. Biol.* **156**, 93-100.
Yang, Y., Mahaffey, C. L., Berube, N., Nystuen, A. and Frankel, W. N. (2005). Functional characterization of fidgetin, an AAA-family protein mutated in fidget mice. *Exp. Cell Res.* **304**, 50-58.
Zhang, D., Rogers, G. C., Buster, D. W. and Sharp, D. J. (2007). Three microtubule severing enzymes contribute to the "Pacman-flux" machinery that moves chromosomes. *J. Cell Biol.* **177**, 231-242.